On the Interaction of Temperature and Magnetic Field in Electromechanical Energy Converters with Permanent Magnets

Flur R. Ismagilov, Viacheslav E. Vavilov, Ilnar I. Yamalov, Vladimir I. Bekuzin

***Abstract*— This paper presents a mathematical description of the electromechanical energy converters with permanent magnets. Unlike well-known mathematical models the mathematical description is obtained by the joint solution of Maxwell and Fourier equations. This allows to determine the geometric dimensions of the active part of electromechanical energy converters taking into account thermal and electromagnetic processes on the stage of the design calculations. Finite element method is used for the final calculations of the full geometry of electromechanical energy converters.**

Computer simulation and experimental study of electric machines with high-coercivity permanent magnets were investigated to evaluate the effectiveness of the obtained results. The results of experimental studies have been compared with mathematical model and its high accuracy was obtained.

***Index Terms*— Electromechanical energy converters, high-coercivity permanent magnets, Magneto-thermal analysis, Fourier equation, Maxwell equations.**

I. Introduction

ELECTROMECHANICAL energy converters (EMEC) with high-coercivity permanent magnet (HCPM) are used in almost all industries: from domestic applications to aerospace engineering [1–4]. This is due to their high reliability and efficiency with minimum weight and overall dimensions.

Therefore, many papers and books are dedicated to the task of design EMEC with HCPM and their design patterns [1-15].

Various mathematical and computer models of EMEC with HCPM obtained by different methods are presented in works [1-15]. Therefore, a mathematical model describing the electromagnetic processes in EMEC with HCPM using the method of magnetic circuits is present in work [1]. Similar mathematical models are presented in [5-7]. The magnetic circuit method is well established in preliminary engineering calculations but the results may differ from the actual characteristics of EMEC by 12-20 %. This divergence is very significant and does not satisfy modern requirements for mathematical models precision. In addition, mathematical models created with the use of magnetic circuits are difficult to apply for studies of dynamic processes and may limit their use.

Various modifications of mathematical models of EMEC with HCPM based on the solution of Maxwell's equations and the vector potential definition are presented in the works [8-12]. These mathematical models have sufficiently high accuracy of magnetic fields calculation and allow to consider dynamic modes of EMEC operation. However, these models only take into account the electromagnetic processes in EMEC with HCPM, i.e. they are narrowly focused, single-disciplinary models. The correct calculation of EMEC with HCPM is not possible without considering the influence of temperature on material properties under electromagnetic calculations as proven in [16-19]. It is also necessary to take into account the effects of rotor speed on the mechanical properties of materials (especially for high-speed and ultra-high-speed EMEC). That is mathematical models satisfying modern requirements should be multi-disciplinary and represent the interdependence at least of the electromagnetic and thermal processes. Single-disciplinary models do not give a complete picture of the processes occurring in EMEC with HCPM. They allow to calculate with sufficient accuracy, right initial conditions and input parameters only one mode of EMEC operation at some point of time or at a very short period of time and at constant environmental conditions.

Papers [13-15] describe mathematical and computer models of EMEC with HCPM obtained by the finite element method with the help of specialized software. These models allow to consider the interconnection of thermal and electromagnetic calculations including transient modes of operation. Multi-disciplinary calculations of these models are implemented in two ways (for example in Ansys software):

– determination of magnetic field distribution in a small time interval (Ansys Maxwell); calculation based on the loss distribution (Ansys Maxwell); calculation on the basis of losses of thermal distribution (Ansys CFX); the allocation of material properties depending on temperature and determination of field distribution for a given temperature. This method is described in [13] and is approximate. In addition it has significant complexity and computational

Manuscript received June 11, 2017; revised June 23, 2017. This work was supported by the Ministry of Education of the Russian Federation under project №8.1277.2017.

F. R. Ismagilov is with the Ufa State Aviation Technical University, Ufa, 450000 Russia (phone: +7-347-273-7787, e-mail: s2_88@mail.ru).

V. E. Vavilov is with the Ufa State Aviation Technical University, Ufa, 450000 Russia (phone: +7-927-3465305, e-mail: s2_88@mail.ru).

I. I. Yamalov is with the Ufa State Aviation Technical University, Ufa, 450000 Russia (phone: +7-919-6001490, e-mail: outlegal@mail.ru).

V. I. Bekuzin is with the Ufa State Aviation Technical University, Ufa, 450000 Russia (e-mail: tiobaldo1@rambler.ru).

requirements.

– Simultaneous calculation of magnetic fields (Ansys Maxwell) and temperature fields (Ansys CFX). This method is quite accurate but the algorithms for this method implementation are just starting to be developed [15]. This method requires significant computer power even when using high-performance computers. It also limits the wide application of this method.

That is why it is very important to develop multi-disciplinary analytical mathematical models of EMEC with HCPM for developing of the General theory of electromechanical energy converters. This model will allow taking into account thermal (with Fourier equations) and electromagnetic (with Maxwell's equations) processes in EMEC and a mechanical processes if necessary.

Generalized structure of a multi-disciplinary mathematical model is presented in figure 1.

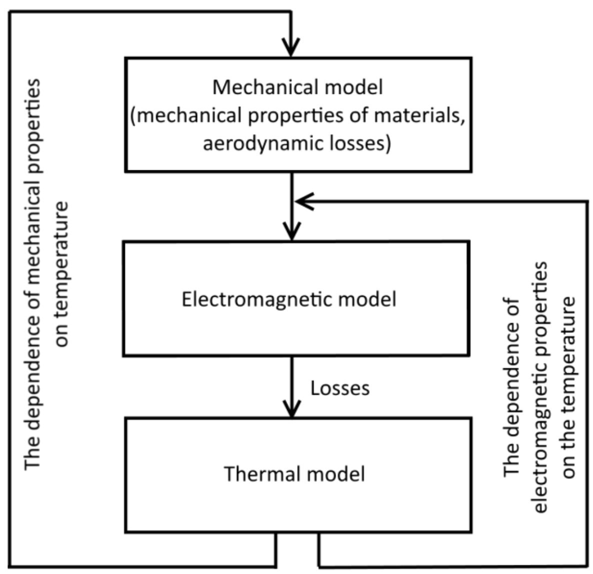

Fig. 1. Structural diagram of multidisciplinary mathematical models.

The full EMEC with HCPM model will be very extensive. Therefore, this work directed to form the basis of generalized multi-disciplinary model of EMEC with HCPM that include accounting interference of magnetic and thermal fields by solving Maxwell's equations and Fourier transforms for the active part of EMEC with HCPM (winding, air gap, permanent magnets). The joint solution of Maxwell's and Fourier equations would fully indicate the physical essence of the interdependence of thermal and electromagnetic processes in EMEC and will allow making numerical magneto-thermal analysis of the EMEC active part without using significant computer power. This will allow to determine the maximum geometric dimensions of the EMEC active part taking into account the thermal and electromagnetic processes at the design calculations stage. The method of finite elements is used for the final geometry calculations of the EMEC.

II. Methodology for Solving the Task

The following assumptions were used to simplify the mathematical transformation:

– Ambient permeability and the air gap permeability are equal to the permeability of vacuum and to the permeability of the magnetic core. The shaft is equal to infinity;

– Stator winding is represented as a thin electrically conductive layer distributed on the bore diameter of the stator magnetic core;

– The induced currents density is constant to the thickness of the thin copper layer;

– Losses of each element are distributed evenly on this item.

– Axial component of the magnetic field at the end of the rotor surface is equal to 0, that is considering infinite length of EMEC;

– The effect of a change in the stator winding resistance on temperature is insignificant and is not taken into account.

Maxwell and Fourier equations are considered in Cartesian coordinates since the ultimate goal is the creation of the generalized mathematical models. In this case the generalized model allows the study of EMEC with HCPM with a cylindrical rotor. Also in this case it is possible to consider the effects of bearing supports (mechanical processes) on the parameters of EMEC. Mechanical processes are mainly considered as the rotor movement along the x and y axes.

Interdependent electromagnetic and thermal processes are considered in solving this problem. Therefore, in mathematical modeling it is necessary to take into account the influence of the cooling system which in this case is taken into account using the heat transfer coefficient. It is assumed in the work that EMEC cooling is carried out on the outer surface of the stator and over the air gap.

The influence of mechanical processes on the parameters of EMEC with HCPM was considered by the authors in [16], therefore they are not considered here. The design scheme is divided into active zones while for each active zone the Maxwell equations (describing electromagnetic processes) and the Fourier equations (describing thermal processes) are solved together.

The Maxwell equations are represented in the form [18]:

$$\mathrm{rot}\vec{H}=\vec{j}+\vec{j}_{\text{ст}},\ \mathrm{rot}\vec{E}=-\frac{\partial\vec{B}}{\partial t},\ \vec{j}=\sigma\left[\vec{E}+\left(\vec{V}\times\vec{B}\right)\right],$$
$$\mathrm{div}\vec{B}=0,\mathrm{div}\vec{j}=0,\ \vec{H}=\mu_0\vec{B}, \qquad (1)$$

where $\vec{B}$ is the magnetic flux density vector of the resulting magnetic field; $\vec{E}$, $\vec{H}$ are electric and magnetic field intensity vector; $\vec{V}$ is the velocity vector of the rotor; σ is the electrical conductivity of the stator winding; $\vec{j}$ is the current density vector; $\vec{j}_{\text{ст}}$ is third-part current density vector.

It is convenient to use the vector potential in studies of the electromagnetic field:

$$\vec{B}=\mathrm{rot}\vec{A}\,. \qquad (2)$$

In the analysis of Maxwell's equations, either Laplace's equations are considered (for zones where there is no current, for example, an air gap), or Poisson's equations (for the zone of permanent magnets and the winding zone). In a general form the vector potential can determined as [18]:

$$\frac{1}{\mu_0}\frac{\partial^2 A_z}{\partial x^2}+\frac{1}{\mu_0}\frac{\partial^2 A_z}{\partial y^2}=0 \quad (3)$$

The mathematical description of permanent magnets is represented as a dependence of the coercive force of the HCPM, remanence induction and magnetization [18]:

$$\vec{B}=\mu\mu_0\left(\vec{M}+\vec{H}\right), \quad (4)$$

where $\vec{M}$ is a magnetization vector of HCPM; μ is a permeability of HCPM.

It is known that the properties of HCPM largely depend on the temperature:

$$B_r(\Theta)=B_{r0}\left(1-\frac{k_{Br}(\Theta_{PM}-20)}{100}\right), \quad (5)$$

$$H_c(\Theta)=H_{c0}\left(1-\frac{k_{Hc}(\Theta_{PM}-20)}{100}\right), \quad (6)$$

$$\mu=\frac{\mu_0 H_{c0}\left(1-\frac{k_{Hc}(\Theta_{PM}-20)}{100}\right)}{B_{r0}\left(1-\frac{k_{Br}(\Theta_{PM}-20)}{100}\right)}. \quad (7)$$

where $B_r(\Theta), H_C(\Theta)$ are the rms value of the remanence induction and coercivity related to flux density of HCPM, respectively; B_{r0}, H_{C0} are respectively the value of the remanence induction and coercivity related to flux density of HCPM specified in the specifications; Θ_{PM} is temperature of HCPM; k_{Br} is temperature coefficient of the remanence induction; k_{Hc} is temperature coefficient of coercivity related to flux density of HCPM.

Then the magnetization of the HCPM depending on the temperature is represented in the form:

$$\vec{M}(x,y,\Theta_{PM})=\frac{B_{r0}^2(x,y)\left(1-\frac{k_{Br}(\Theta_{PM}-20)}{100}\right)^2}{\mu_0^2 H_{c0}(x,y)\left(1-\frac{k_{Hc}(\Theta_{PM}-20)}{100}\right)}-H_{c0}(x,y)\left(1-\frac{k_{Hc}(\Theta_{PM}-20)}{100}\right) \quad (8)$$

The Fourier equations for each considered zone have their interpretation: for isotropic and anisotropic bodies. For isotropic bodies with an internal source of heat (stator winding, rotor bandage, not laminated shaft) [19]:

$$\frac{d\Theta}{dt}=\frac{\lambda}{c\rho}\left(\frac{\partial^2\Theta}{\partial x^2}+\frac{\partial^2\Theta}{\partial y^2}+\frac{\partial^2\Theta}{\partial z^2}\right)+\frac{q_v}{c\rho}, \quad (9)$$

where Θ is body temperature; q_v is specific thermal power flow of internal source; c is specific heat capacity; λ is thermal conductivity.

For anisotropic bodies [19]:

$$\frac{d\Theta}{dt}=\frac{1}{c\rho}\left(\lambda_x\frac{\partial^2\Theta}{\partial x^2}+\lambda_y\frac{\partial^2\Theta}{\partial y^2}+\lambda_z\frac{\partial^2\Theta}{\partial z^2}+q_v\right). \quad (10)$$

III. Accounting of Mutual Influence of Magnetic and Thermal Fields in EMEC with HCPM

Stationary magnetic and thermal fields are considered in the analysis of mutual influence of thermal and magnetic fields. It is important to note that all the presented solutions are available for dynamic modes. This is considered in the block diagram, figure 2.

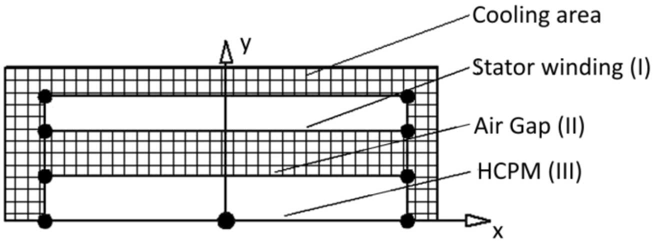

Fig. 2. EMEC with HCPM calculation scheme.

The Fourier equation of Zone I (winding zone) for a three-dimensional field is determined as:

$$-\frac{q_{vcu}}{\lambda_{cu}}=\frac{\partial^2\Theta_{Cu}}{\partial x^2}+\frac{\partial^2\Theta_{Cu}}{\partial y^2}+\frac{\partial^2\Theta_{Cu}}{\partial z^2}, \quad (11)$$

where Θ_{cu} is winding temperature; q_{vcu} is specific thermal power flow of winding; λ_{cu} is thermal conductivity of winding.

It is obvious that the specific heat power of the winding is determined by:

$$q_{vcu}=\frac{j_z^2}{\sigma}. \quad (12)$$

Then, substitute the expression (11) by expression (13):

$$-\frac{j_z^2}{\lambda_{cu}\sigma}=\frac{\partial^2\Theta_{cu}}{\partial x^2}+\frac{\partial^2\Theta_{cu}}{\partial y^2}+\frac{\partial^2\Theta_{cu}}{\partial z^2}. \quad (13)$$

In general:

$$-j_z\frac{j_z}{\lambda_{cu}\sigma}=\nabla^2\Theta_{cu}. \quad (14)$$

The vector potential equations for zone I:

$$\frac{1}{\mu_0}\frac{\partial^2 A_z}{\partial x^2}+\frac{1}{\mu_0}\frac{\partial^2 A_z}{\partial y^2}=-j_z. \quad (15)$$

Combining (14) and (15):

$$\frac{j_z}{\lambda_{cu}\sigma}\left(\frac{1}{\mu_0}\frac{\partial^2 A_z}{\partial x^2}+\frac{1}{\mu_0}\frac{\partial^2 A_z}{\partial y^2}\right)=\frac{\partial^2\Theta_{cu}}{\partial x^2}+\frac{\partial^2\Theta_{cu}}{\partial y^2}+\frac{\partial^2\Theta_{cu}}{\partial z^2}\cdot \quad (16)$$

Since the EMEC of infinite length then $\frac{\partial^2\Theta_{cu}}{\partial z^2}=0$.

$$\frac{\partial^2\Theta_{cu}}{\partial x^2}-\frac{j_z}{\lambda_{cu}\sigma\mu_0}\frac{\partial^2 A_z}{\partial x^2}+\frac{\partial^2\Theta_{cu}}{\partial y^2}-\frac{j_z}{\lambda_{cu}\sigma\mu_0}\frac{\partial^2 A_z}{\partial y^2}=0\cdot \quad (17)$$

Thus, expression (17) shows the interdependence of magnetic and thermal fields. Then the dependence of the EMEC parameters on the mechanical processes of the rotor (oscillations, vibrations, etc.) is revealed introducing the velocity vector in expression (17) and expanding it along the coordinates. Also expression (17) demonstrates the connection between the laws of electromagnetism described by the Maxwell equations and the heat equation (Fourier equations). It can be concluded from expression (17) that these thermal and magnetic fields must be considered only together. And in expression (17) there are no temperature-dependent materials (the dependence of the winding resistance on temperature is neglected).

The solution of equation (17) is possible only by numerical methods. It can also be solved by a separate analysis (13) and (15) after which their solutions can be equated.

It is expedient to use boundary conditions of the third kind for temperature fields and the method of separation of variables to solve equation (13). In this case the Fourier equation can be written as follows:

$$\begin{aligned}&\frac{\partial\Theta_{cu}}{\partial x}+\frac{\alpha}{\lambda_{cu}}\Big|_{x=x_1}=0\\&\frac{\partial\Theta_{cu}}{\partial y}+\frac{\alpha}{\lambda_{cu}}\Big|_{y=y_4}=0\end{aligned}. \quad (18)$$

Due to the symmetry of the thermal field:

$$\begin{aligned}&\frac{\partial\Theta_{cu}}{\partial x}\Big|_{x=0}=0\\&\frac{\partial\Theta_{cu}}{\partial y}\Big|_{y=0}=0\end{aligned}, \quad (19)$$

where α is heat transfer coefficient for the cooling surface.

Taking into account (18) and (19) the solution (13) is known and described in various papers. The boundary conditions and solutions with their allowance for (15) are described in [18]. Thus, it is clear that a generalized solution of (17) is possible and can be used for practical calculations.

Further, it seems reasonable to consider Zone III (HCPM). The magnetization of permanent magnets takes place in zone III and eddy currents are induced in permanent magnets creating losses in them. Then the vector potential equation for zone III can be represented taking into account the temperature dependence of the magnetization as:

$$\frac{1}{\mu_0}\frac{\partial^2 A_z}{\partial x^2}+\frac{1}{\mu_0}\frac{\partial^2 A_z}{\partial y^2}=-j_{zpm}+\frac{\partial M\left(\Theta_{PM}\right)_x}{\partial y}-\frac{\partial M\left(\Theta_{PM}\right)_y}{\partial x}. \quad (20)$$

The Fourier equation for zone III:

$$-q_{vpm}=\lambda_{pmx}\frac{\partial^2\Theta_{PM}}{\partial x^2}+\lambda_{pmy}\frac{\partial^2\Theta_{PM}}{\partial y^2}+\lambda_{pmz}\frac{\partial^2\Theta_{PM}}{\partial z^2}, \quad (21)$$

where Θ_{PM} is HCPM temperature; q_{vcu} and q_v are specific thermal power flow of HCPM; $\lambda_{pmx},\lambda_{pmy},\lambda_{pmz}$ are HCPM thermal conductivity along different axes.

It is necessary to take into account that the HCPM has temperature anisotropy when solving the equation (21). For the HCPM based on the SmCo alloy the thermal conductivity along the axes can differ 2-4 times and more then 5 times for NdFeB.

The specific thermal power flow of the HCPM is determined by:

$$q_{vcu}=\frac{j_{zpm}^2}{\sigma_{PM}}\cdot \quad (22)$$

By analogy with expression (13) expressions (20) and (21) can be written together:

$$\left(\frac{1}{\mu_0}\frac{\partial^2 A_z}{\partial x^2}+\frac{1}{\mu_0}\frac{\partial^2 A_z}{\partial y^2}-\frac{\partial M\left(\Theta_{PM}\right)_x}{\partial y}+\frac{\partial M\left(\Theta_{PM}\right)_y}{\partial x}\right)\frac{j_{zpm}}{\sigma_{PM}}=\lambda_{pmx}\frac{\partial^2\Theta_{PM}}{\partial x^2}+\lambda_{pmy}\frac{\partial^2\Theta_{PM}}{\partial y^2}, \quad (23)$$

or:

$$\begin{aligned}&\lambda_{pmx}\frac{\partial^2\Theta_{PM}}{\partial x^2}+\lambda_{pmy}\frac{\partial^2\Theta_{PM}}{\partial y^2}-\frac{j_{zpm}}{\sigma_{PM}\mu_0}\frac{\partial^2 A_z}{\partial x^2}-\frac{j_{zpm}}{\sigma_{PM}\mu_0}\frac{\partial^2 A_z}{\partial y^2}+, \quad (24)\\&+\frac{j_{zpm}}{\sigma_{PM}\mu_0}\frac{\partial M\left(\Theta_{PM}\right)_x}{\partial y}+\frac{j_{zpm}}{\sigma_{PM}\mu_0}\frac{\partial M\left(\Theta_{PM}\right)_y}{\partial x}=0\end{aligned}$$

It can be seen from expression (24) that zone III in contrast to zone I has an extremely complex interdependence of temperature and magnetic fields. As seen from (24) this complexity is characterized by a complex process which is caused by the initial effect of magnetization on the temperature of the HCPM. This in turn subsequently affects magnetization which subsequently affects the temperature of the HCPM, etc. These processes can continue many times until a steady temperature is reached.

The boundary conditions that apply to the expressions (21), (23) and (24) are similar to expressions (18) and (19), except the constancy of temperature conditions are specified on the boundary of the HCPM (boundary conditions of the first kind).

Thus, it is obvious that the expressions (17) and (24) describe the heat exchange between the active elements of the EMEC, the heating of the EMEC due to the losses, the electromagnetic characteristics of the EMEC and the interdependence of the thermal and magnetic fields of the EMEC.

The most difficult problem is evaluation of the interdependence of fields for the zone II (air gap). In this case the equation for the vector potential is taken as:

$$\frac{1}{\mu_0}\frac{\partial^2 A_z}{\partial x^2}+\frac{1}{\mu_0}\frac{\partial^2 A_z}{\partial y^2}=0\cdot \qquad (25)$$

The Fourier equation for zone II:

$$\frac{-q_{vair}}{\lambda_{air}}=\frac{\partial^2\Theta_{air}}{\partial x^2}+\frac{\partial^2\Theta_{air}}{\partial y^2}+\frac{\partial^2\Theta_{air}}{\partial z^2}, \qquad (26)$$

where Θ_{air} is temperature of air gap; q_{vair} is specific thermal power flow in air gap; λ_{air} is thermal conductivity of air.

In this case specific heat power is determined not by electromagnetic fields but by the mechanical characteristics of EMEC: rotation frequency, friction coefficient, rotor diameter and air gap size.

Therefore, the interdependence of the thermal and electromagnetic fields in the air gap characterized by the boundary conditions at determined from the solution of equations (17) and (24). When solving these equations the temperatures are determined at the boundaries y = y3 and y = y2 which are established by the interdependence of the magnetic and thermal fields. It is important to note here that the air gap area is the main area for taking into account the mechanical processes (rotor dynamics, mechanical strength and aerodynamic losses).

Therefore, based on the boundary conditions the interdependence of thermal and magnetic fields in the air gap is represented implicitly and is determined indirectly. In an explicit form can separately show the dependence of mechanical and thermal or magnetic and mechanical fields in the air gap.

To fully evaluate these interdependencies it is necessary to take into account the speed and displacement of the rotor in expressions (17) and (24). These models were investigated by authors in [16].

Thus, a mathematical apparatus for investigating the mutual influence of the magnetic and thermal fields of EMEC with HCPM is formulated on the basis of a joint analysis of the Maxwell and Fourier equations. This makes possible to significantly improve the accuracy of EMEC design calculations with HCPM.

IV. The Practical Application of the Developed Method of Evaluation of the Mutual Influence of Magnetic and Thermal Fields

To evaluate the effectiveness of the research it seems appropriate to assess the results for a specific numerical example. The efficiency evaluation is performed on a synchronous motor with permanent magnets (SMPM) and direct starting.

This type of a motor is widely used in aircraft, oil and gas industry, etc.

Figure 3 shows a general view of the SMPM. The SMPM rotor is a combined EMEC: asynchronous motor and EMEC with HCPM. This gives main advantages and main disadvantages to EMEC: they are able to run without special electronics; they have a higher coefficient of efficiency and cosφ as compared to asynchronous motors. At the same time, due to the presence of permanent magnets during start-up SMPM has synchronous braking torque, which greatly reduces the SMPM starting torque. Therefore, this EMEC has lower starting torque compared to asynchronous or synchronous EMEC with soft start.

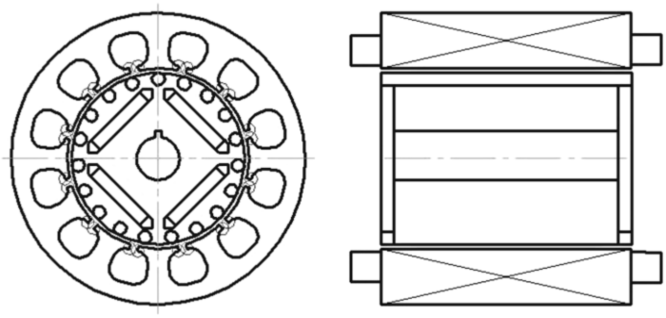

Fig. 3. SMPM general view.

Obviously, under the influence of losses in the rotor (EMEC operates in an asynchronous mode, the losses in the rotor are considerable) permanent magnets are heated at the start of the SMPM. According to expression (5)-(7) their characteristics decrease. This leads to the braking synchronous torque reduction. The known design techniques of SMPM do not take this into account which leads to an underestimation of the calculated starting torque and incorrect selection of the SMPM parameters.

This research allows to take into account these physical features of EMEC.

Therefore, the starting torque of SMPM was calculated with the parameters presented in Table 1 using the Ansys Maxwell software. Moment characteristics calculated by this method are shown in Fig. 4.

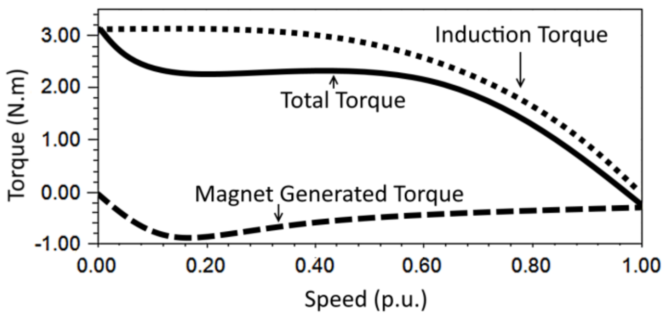

Fig. 4. The calculation of the torque characteristics of the SMPM excluding heating HCPM.

As can be seen from figure 4 the minimum starting torque of SMPM is 2.1 Nm at 20% of the nominal speed. According to these calculations SMPM for selected geometric dimensions does not allow to achieve the necessary moment characteristics.

Taking into account the losses in the rotor and using the developed mathematical model the temperatures of permanent magnets equal to the 60 ºC were obtained. The time constant for the heating of permanent magnets in SMPM is small since the thickness of the HCPM is not more than 3 mm. Therefore, this temperature was reached at 0.2 sec.

TABLE I
SMPM CHARACTERISTICS

Power, kW	1,1
Rotational speed, rpm	12000
Phase / linear voltage, V	115/200
Number of poles	4
Power frequency, Hz	400
Current, A	3,02
Efficiency	83
Power factor	0,81
EMF (phase)	83,8
Acceleration time to the rated rotor speed, ms	200
Required starting torque at 20% rated speed, Nm	2,5
Current density, A/mm^2	14,8
Linear load, A/m	21775
Number of slots stator / rotor	36/32
Steel grade / thickness of stator sheets, mm	2421/0,35
Steel grade / thickness of rotor sheets, mm	2421/0,35
Stator wire, make / size, mm	Polyimide insulation wire / 0,6
Winding type	Distributed
Number of layers / parallel branches	1
Number of elementary wires per conductor	1
Number of phases / poles	3/4
Step winding through the slot	7
Number of parallel conductors in the turn	1
Number of conductors in the slot	19
Approximate winding overhang, mm	19
Straight line of winding overhang, mm	15
Active phase resistance at 20 °C, Ohm	1.71254
Active resistance in the terminals of short-circuiting winding at 20 °C, Ohm	1.18711e-005
Inductance Xd / Xq, mH	8427/16040
Magnet brand / height of magnets, mm	Sm_2Co_{17} / 3
Residual flux density at 20 °C, T	1,01
Coercive force at 20 ° C, A / cm	756
Magnetic flux density in the gap, T	0,32
Magnetic flux density in the stator teeth, T	0,68
Magnetic flux density in the stator back, T	0,99

Figure 5 shows the calculation of the moment characteristics. It can be seen that the resulting torque at 20% of the rated speed increases by 0.5 Nm. In this case the geometric dimensions of the SMPM satisfy the requirements.

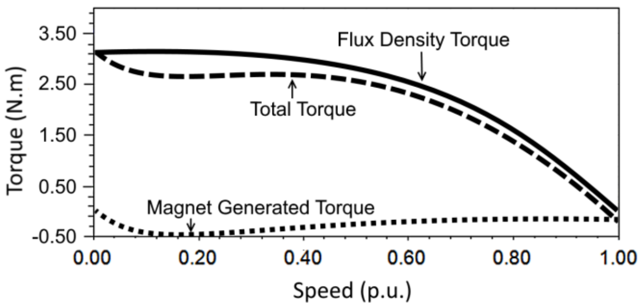

Fig. 5. The calculation of moment characteristics of SMPM taking into account heating of HCPM.

It is important to note that the calculated results are confirmed by the results of experimental studies carried out at the Department of Electromechanics of Ufa State Aviation Technical University. Figure 6 shows the experimental SMPM model and the rotor of the experimental SMPM.

To simplify laboratory tests in experimental studies the characteristics of SMPM were investigated in the generator mode (which is only the starting braking torque created by permanent magnets was investigated).

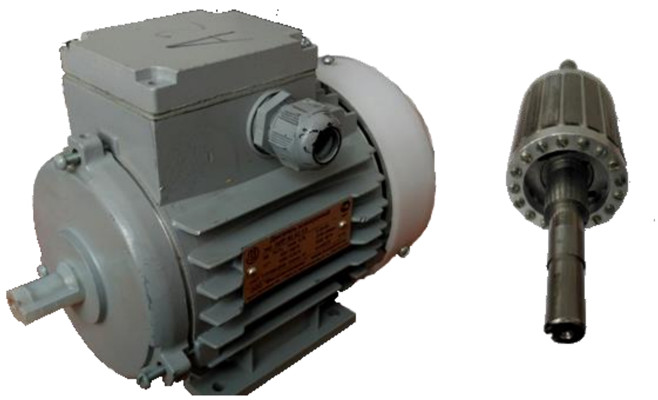

Fig. 6. The SMPM model and the SMPM rotor.

Rotating speed and idle EMF relation were obtained by the experimental SMPM technique consisted in the fact that the SMPM was accelerated in the generator mode to a rotating speed of 3000 rpm. Based on the magnitude of the EMF in the generator mode the braking torque of the SMPM is determined. After that the SMPM was accelerated with the help of an asynchronous start-up in the engine mode up to 3000 rpm. Thus, the rotor is warmed up. After that the SMPM is started again in the generator mode and the decrease of idling EMF and heating of the HCPM is estimated.

The results of the experimental studies are shown in Fig. 7.

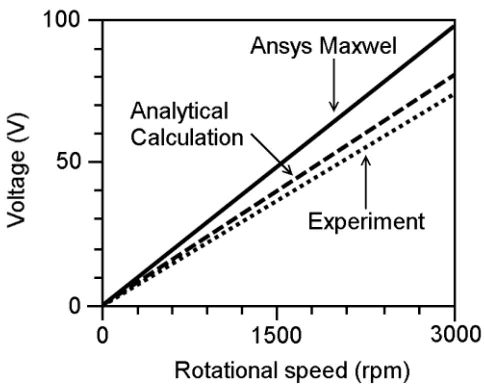

Fig. 7. The experimental studies results.

Taking into account the heating of the HCPM it can be seen from the experimental studies that the braking moment of SMPM has a lower value (by 20%) than without heating. That is, without taking into account the interdependence of thermal and electromagnetic processes.

Numerical example and the results of experimental studies prove the feasibility of the theoretical studies carried out.

The conducted research allow to form a new method of calculating the SMPM at the start. The results of the studies shows that the characteristics and the dimensions of HCPM should be chosen in a way to maximize the temperature of SMPM at the start and minimize a magnetic field generated by them. This allow to receive in SMPM the maximum starting moment with the minimum counter EMF. The losses in the SMPM rotor will decrease as it accelerates and synchronizes, and the temperature of the permanent magnets will also decrease. This will allow to achieve maximum torque in the synchronous mode of SMPM. This method may have significant practical effect.

Also, to study the mutual effects of thermal and electromagnetic processes in EMEC with HCPM, calculations were made not only for SMPM, but also for a high-speed permanent magnet generator. As a result of these calculations the dependences of the magnetic flux radial component in the air gap of the high-speed EMEC with HCPM on the temperature, the air gap size and the characteristics of the applied HCPM were obtained.

Analysis of these dependences showed that with an increase in the air gap, the amplitude of the radial component of the magnetic flux decreases by 1.85 times, and with an increase in the air gap by 28.5%, the amplitude of the radial component of the magnetic flux in the air gap EMEC with HCPM is reduced by 66% .

In these studies, constant temperature coefficients were used for HCPM of various grades and it was found that the HCPM temperature had a significant effect on the magnetic flux radial component in the air gap. Therefore, for NdFeB HCPM with increasing temperature from 70°C to 140°C the radial component of the magnetic flux is reduced by 25-35%. At a temperature of 230°C, the initial characteristics of NdFeB 38UH are larger by more than 10% for residual induction by more than 10% for Sm2Co17, and for coercive force by 7-8%, NdFeB 38UH creates a radial magnetic flux of 9% more than Sm2Co17. At a temperature of 140-150°C, Sm2Co17 HCPM creates a magnetic flux in the air gap EMEC with HCPM by 20% more than NdFeB 38UH. At a temperature of 700°C, the characteristics of Sm2Co17 HCPM and NdFeB 38UH become equal and create the same magnetic flux. Thus, in EMEC with HCPM, it is advisable to use NdFeB HCPM at a temperature of no higher than 500°C, in other cases it is more appropriate to use Sm2Co17 HCPM in terms of energy performance.

V. CONCLUSION

Thus, in the article the mathematical apparatus, that allowed to estimate mutual influence of magnetic and thermal fields in EMEC with HCPM, is developed. The assumptions and boundary conditions for carrying out theoretical studies of these equations are established. The need to consider the interdependence of magnetic and thermal EMEC with HCPM in the design on a numerical example with experimental confirmation is justified. Experimental studies confirming the accuracy of the developed mathematical model were carried out.

On the basis of our studies, the limits of the use of various permanent magnet brands as a function of temperature have been determined. In EMEC with HCPM, it is advisable to use NdFeB HCPM at a temperature of no higher than 500°C, in other cases it is more appropriate to use Sm2Co17 HCPM in terms of energy performance. This conclusion is of a general nature for various types of EMEC with HCPM.

As a result of the conducted studies, a new method for calculating SMPM was proposed using the developed mathematical model.

ACKNOWLEDGMENT

The work was supported by the Ministry of Education of the Russian Federation, project №8.1277.2017.

REFERENCES

[1] W. Kemmetmüller, D. Faustner, A. Kugi, "Modeling of a permanent magnet synchronous machine with internal magnets using magnetic equivalent circuits," *IEEE Trans. Magn.*, vol. 50, no. 6, pp. 1-14, 2014.

[2] Li W., X. Zhang, S. Cheng, "Thermal Optimization for a HSPMG Used for Distributed Generation Systems," *IEEE Transactions on Industrial Electronics,* vol. 60, no. 2. pp. 474-482, 2013.

[3] Zhongda Tian, Shujiang Li, Yanhong Wang, and Quan Zhang, "Multi Permanent Magnet Synchronous Motor Synchronization Control based on Variable Universe Fuzzy PI Method," *Engineering Letters*, vol. 23, no.3, pp. 180-188, 2015.

[4] P. Pao-la-or, A. Isaramongkolrak, T. Kulworawanichpong "Finite Element Analysis of Magnetic Field Distribution for 500-kV Power Transmission Systems," *Engineering Letters*, vol. 18, no.1, pp. 1-9, 2010.

[5] A. R. Tariq, C. E. Nino-Baron, and E. G. Strangas, "Iron and magnet losses and torque calculation of interior permanent magnet synchronous machines using magnetic equivalent circuit," *IEEE Transactions on Magnetics*, vol. 46, pp. 4073-4080, 2010.

[6] J. Tangdu, T. Jahns, and A. El-Refaie, "Core loss prediction using magnetic circuit model for fractional-slot concentrated-winding interior permanent magnet machines," *IEEE Energy Conversion Congress and Exposition*, pp. 1004–1011, 2010.

[7] B. Sheikh-Ghalavand, S. Vaez-Zadeh, and A. H. Isfahani, "An improved magnetic equivalent circuit model for iron-core linear permanent-magnet synchronous motors," *IEEE Transactions on Magnetics*, vol. 46, pp. 112–120, 2010.

[8] Z. Q. Zhu, K. Ng, N. Schofield, and D. Howe, "Improved analytical modelling of rotor eddy current loss in brushless machines equipped with surface-mounted permanent magnets," *IEE Proc.—Elect. Power Appl.*, vol. 151, no. 6, pp. 641-650, 2004.

[9] S. R. Holm, "Modelling and Optimization of a Permanent Magnet Machine in a Flywheel," *Ph.D. dissertation*, Technische Universiteit, Delft, 2003.

[10] M. Markovic and Y. Perriard, "Analytical solution for rotor eddy-current losses in a slotless permanent-magnet motor: The case of current sheet excitation," *IEEE Trans. Magn.*, vol. 44, no. 3, pp. 386-393, 2008.

[11] M. Markovic and Y. Perriard, "An analytical determination of eddycurrent losses in a configuration with a rotating permanent magnet," *IEEE Trans. Magn.*, vol. 43, no. 8, pp. 3380-3386, 2007.

[12] Y. N. Zhilichev, "Analytic solutions of magnetic field problems in slotless permanent magnet machines," *Int. J. Comput. Math. Elect. Electron. Eng.*, vol. 19, no. 4, pp. 940-955, 2000.

[13] Vilijan MATOŠEVIĆ, Željko ŠTIH Uljanik TESU d.d "2D Magneto-thermal analysis of synchronous generator," *Przegląd elektrotechniczny*, vol. 90, pp. 157-160, 2014.

[14] J. Driesen, R. Belmans, K. Hameyer, "Methodologies for coupled transient electromagnetic-thermal finite element modeling of electrical energy transducers," *IEEE International Electric Machines and Drives Conference* 939387, pp. 681-686, 2001.

[15] Zhang, Xiaochen and Li, Weili and Baoquan, Kou and Cao, Junci and Cao, Haichuan and Gerada, C. and Zhang, He "Electrothermal combined optimization on notch in air-cooled high-speed permanent-magnet generator," *IEEE Transactions on Magnetics*, vol. 51, no. 1, pp.1-10, 2015.

[16] Ismagilov, F.R., Khayrullin, I.H., Vavilov, V.E., Yakupov, A.M. "Generalized mathematic model of electromechanical energy transducers with non-contact bearings," *Engineering Letters,* vol. 25, no. 1, pp. 30-38, 2017.

[17] Dajaku, G.: "Electromagnetic and thermal modeling of highly utilized PM machines," *Ph. D. Thesis,* University of Federal Defence Munich, Institute for Electrical Drives and Actuators, 2006.

[18] Pierre-Daniel Pfister, Yves Perriard Slotless "Permanent-Magnet Machines: General Analytical Magnetic Field Calculation," *IEEE Transactions on Magnetics*, vol. 47, no. 6, pp. 1739-1752, 2011.

[19] LI Wei Li Zhang Xiao Chen, Cheng Shu Kang Cao Jun Ci Zhang Yi Huang "Thermal analysis of high speed permanent magnetic generator," *Technological Sciences,* vol. 55, no. 5, pp. 1419-1426, 2012.

Flur R. Ismagilov – Prof., Head of the Department of Electromechanics, Ufa State Aviation Technical University (Ufa), phone: +7-347-2737787
Vacheslav E. Vavilov – P.h.D., Lecturer of the Department of Electromechanics, Ufa State Aviation Technical University (Ufa), phone: +7-927-3465305, e-mail: s2_88@mail.ru.
Ilnar I. Yamalov – P.h.D., Lecturer of the Department of Electromechanics, Ufa State Aviation Technical University (Ufa), phone: +7-919-6001490, e-mail: outlegal@mail.ru
Vladimir I. Bekuzin– Post-graduate student, Engineer at the Department of Electromechanics, Ufa State Aviation Technical University (Ufa).